THE DESIGN AND DEVELOPMENT OF A SELF-COMMUTATING STEPPER MOTOR

By K.R. Dalley M.Sc.

Marconi Space & Defence Systems Ltd., Frimley, Surrey, U.K.

ABSTRACT

This paper is the result of a M.Sc. Project ref. 1 carried out by the author in co-operation with Marconi Space and Defence Systems Ltd (MSDS) and the University of Surrey. The Project established that a self-commutating (s.c.) stepper motor could be used as a high speed d.c. brushless motor. The system discussed adopts a well established and space proven motor, the 'stepper-motor' and shows that with simple commutation techniques it can be operated as a Brushless d.c. motor at high speeds (>10,000 rpm).

1.0 INTRODUCTION

The design of this particular motor has been developing over the past 5 years and was successfully put into practice during a system study of a Temperature Sounding Radiometer for a Geostationary Meteorological Satellite ref 2. The motor was controlled by LED/Photodiodes pulsed by a shutter attached to the rotor and maintained 2000 rpm with speed control of 0.06%. Recently another system was developed where the stepper motor was controlled by reed-switches. These were activated by static magnets shunted by an iron shutter attached to the motor shaft. However, both these applications were at relatively low speeds. The M.Sc. project undertaken by the author extended the knowledge of the reed-switch concept and concluded with the development of a self-commutating motor capable of 20,000 rpm. During the development program two unique stepper motor concepts were introduced. These were to operate a 'stepper' with continuous voltages greater than the recommended drive voltage and at speeds in excess of the 'drop-out' pulse rate. The final design comprised a Moore Reed Co. Ltd, size 15, 4-phase permanent magnet*(p.m.) stepper motor incorporating Hall Effect elements for its commutation.

2.0 PRINCIPLE OF THE SELF-COMMUTATING STEPPER

Although the stepper is essentially a position control device, the ability to rotate a load rapidly through large angles requiring many incremental steps is a common requirement. Previously the conventional method of driving a stepper motor at high speeds was to increase the drive frequency, until the step rate is in synchronism with the drive frequency. However, there are two operational limitations when adopting this drive technique. The motor will only start if the drive frequency is within the 'response range'. Then if greater step rates are required the drive frequency must be increased as a ramp function. The motor is now said to be in its 'slew range', but a further limit is then imposed as the motor eventually losses synchronism at the 'drop-out' rate

* The p.m. motor discussed within the context of this paper is as defined by British motor manufacturers; in that the rotor consists of a 2 pole magnet and is not toothed.

(typically 5000 rpm). However in the s.c. stepper, the motor is not frequency driven but like the d.c. motor the speed is proportional to the voltage applied across the motor winding. The motion of the rotor with respect to the stator is controlled by self-generated switching of the stator windings. If one of the stator windings is energised then the rotor will step to its magnetic equilibrium point. If now on immediately acquiring this equilibrium point the next winding is energised then the rotor will continue to the next equilibrium point. If now again the next winding is immediately energised the process will continue and the rotor will rotate as if a velocity drive. The switching is controlled by encoding the position of the rotor and is therefore described as 'self-commutating'. An important feature of this drive technique is that the self-commutated stepper operated at speeds greater than the 'drop-out' rate.

3.0 THE SELF-COMMUTATING STEPPER

3.1 Commutation: Brushless motors can be driven in either a switching or a proportional mode. The principle advantage of the proportional drive is the elimination of generated torque ripple. However, as the stepper motor has been optimally designed to drive in a switched mode, this mode was adopted for the self-commutating stepper. Early experiments were carried out upon the stepper to establish an optimum drive mode. The performance of the stepper was found to be significantly dependant upon which of the 3 principle energisation modes A, B or AB were adopted. Mode A is when only one phase at a time is energised, whereas mode B is when two phases are energised at any one time. In both cases the motor executes one basic step for each input pulse. A combination of A and B in which the motor phases are energised sequentially in mode A followed by B is known as AB. In this mode, the motor will execute half of the basic step. The number preceding the mode letter defines the number of motor phases to which the mode applies. As a 4 phase, size 15 stepper was readily available for the author's M.Sc. project, the investigation was only concerned with the 4A, 4B and 4AB modes. The tests were carried out using a reed-switch system having an inertial load of 1×10^{-5} Kgm^2. Measurements were made at various speeds between 2000 and 12000 rpm. A summary of the results from these tests is presented in figures 1 and 2. It can be seen that the 4A mode required the least input power and that a phase advance of 45° further improved the overall performance. A study of various torque waveforms demonstrated that the value of the mean torques predicted the above experimental results.

3.2 Rotor position sensors: There are a variety of devices commercially available as rotor position sensors. However, only non-contacting sensors were considered as only these ensured long operational life and reliability. The principle types reviewed were (a) capacitive; (b) inductive; (c) optical and (d) Hall effect elements. Capacitive devices although having low power were considered unreliable for satellite applications. Inductive sensors such as proximity switches, variable electronics devices and variable transformers were eliminated as they either required complex circuitry for excitation and demodulation, or because they required a moving magnetic field were therefore not self-starting. An exception to this was the magnetic relay (reed-switch) see fig. 3. This concept comprises 4 equally spaced reed-switches, each activated by 4 static magnets which are shunted by a rotating iron shutter attached to the rotor. If the gap in the shunt is 90 degrees then at any

instant of time only one relay is energised and this constitutes a 4A mode. The advantages of the reed-switch is that it acts as both sensor and commutator and therefore requires no additional components. Unfortunately because of low contact operation life, the reed-switch concept is only suitable for low speed or short life applications (≤ 2000 rpm). The Optical sensor, in its simplest form is a disc attached to the rotor. The disc carries a reflective track that provides the same function as the shunt gap in the reed switch system. A fixed light source is reflected by the track onto a photo-sensitive device whose output is used to generate the switching signal. However the reliability of optical devices in a space environment is again doubtful. Two Hall effect transducers were investigated, the magneto-resistor and the Hall Effect Element. Both are semiconductor devices capable of detecting a magnetic field similar to the reed-switch concept. However, the Hall effect element has one unique property, it can distinguish between north and south poles of a magnet. This property means that only two sensors are required to provide the necessary commutation. The shape of the Moore Reed rotor magnet is particularly appropriate as it provides the 90 degree commutation angle required for a 4A energisation mode. The Hall Effect Element commutator fig. 4 was chosen for the optimum design because of its reliability, low power consumption, and that it did not require an additional commutation disc.

3.3 Drive Techniques: The emphasis during the design of the drive amplifiers was to keep the complexity of the electronics to a minimum. Ideally the reed-switch technique achieved this design aim, but because of unreliability at high speeds a transistor drive had to be adopted. The s.c-drive amplifiers can be divided into two basic types, (a) the Unipolar, and (b) the Bipolar amplifier. The Unipolar drive is defined as an amplifier were the drive voltage is from a single polarity supply. The motor windings are usually arranged such that the centre-taps form a 'star point' and each of the remaining winding terminals are then energised in the appropriate sequence depending on the drive mode. The Bipolar technique is here defined as an amplifier which adopts both positive and negative voltage supplies. The motor winding centre-tap is not required in this technique, but the current reversal requires the use of a bridge amplifier. The use of a dual voltage level amplifier sometimes referred to as Bipolar was not considered a suitable technique in velocity control applications. Although during the comparison it was found that the Bipolar amplifier was the more efficient it required twice the number of components and therefore the Unipolar drive was chosen for the optimum circuit. The drive circuit is shown in fig. 5. As the motor was tested up to a maximum voltage of 60 volts a current limit was necessary to prevent over-current drive causing demagnetisation of the p.m. magnet. It is usual to have a protection diode across the output transistor collector/emitter junctions to prevent the back-emf spike damaging the output transistor. However in the case of the s.c-stepper this diode would also suppress the back-emf voltage of the unenergised coils. The requirement to protect the output transistors and still maintain the back-emf was achieved by connecting Zenar Diodes in series with the diode. The value of the Zenar being determined by the output transistor Vce max. As the requirements for the output transistors was that the Vce max must be twice the drive voltage only NPN transistors were found available. The required motor drive voltage was only applied to the output transistor and the rest of the circuit operated from a low voltage rail.

3.4 Feedback Techniques: The design criteria for the feedback transducer was to keep the concept simple. Traditional methods such as commercially available tachometers were not considered for this application as they would introduce a further inertial load to the motor shaft. Two feedback techniques were studied during the project, both of which utilised existing waveforms within the self-commutating motor and therefore required no additional hardware. The first method used the output from any one of the position sensors. A frequency to analogue converter would then produce a dc voltage proportional to either speed or error. The second method utilised the internal back-emf voltage developed in the unenergised windings of the stepper. The generated back-emf is sensed in all four windings by four diodes. These diodes provide a low impedance path for the induced reverse currents. The currents are then summed in a resistor. The voltage drop across this resistor, when suitably smoothed, provides a d.c. signal proportional to the rotor angular velocity. This latter method proved to be the most effective and simpler of the techniques.

3.5 Motor Performance: Several performance tests were carried out on an unloaded motor shown in Fig. 6 using a standard manufacturers test jig (courtesy of the Moore Reed Co. Ltd.) The measurements of Torque against speed and input current mode are presented in figures 7 and 8. Other measurements made included back-e.m.f., efficiency, performance in vacuum and motor friction. A summary of the motor parameters measured is given in the table below.

Motor type		Size 15, 4 phase p.m. stepper
Drive mode		4A self-commutating
Peak torque		140 gm cm.
Volts at peak torque		28 volts
Amps at peak torque		0.4 amp
Torque sensitivity		0.034 Nm. amp^{-1}
Motor Friction torque		6.4×10^{-5} Nm.
No-Load speed in air	V = 28V	7000 rpm
	V = 60V	12500 rpm
No-Load speed in vacuum	V = 60V	31600 rpm
Power consumption in vacuum	1.7 watts at 20,000 rpm	
	0.1 watt at 5,000 rpm	
Efficiency	>70%	

During these tests it was noticed that a phase shift of 45 degrees did not provide the maximum motor speed for a fixed voltage. Further investigations showed that the no-load speed could be increased if the phase advance was increased to 90 degrees, at a cost of increased input power and loss of efficiency. This improved speed was attributed to the relationship between the drive pulse and the peak of preceeding motor winding's back-emf waveform. Further increases in no-load speed were later achieved by operating the motor in a pseudo-4AB mode. This was achieved by adjusting the Hall Effect Element control current. Again the increase in speed was at a cost of increased power consumption of both the drive circuit and motor. A No-load speed of 31,600 rpm was recorded when operating in this pseudo-4AB drive mode.

4. SIMULATION MODEL

During the project a mathematical model was developed to describe the dynamic characteristics of the s.c-motor. The objective was to obtain a system of differential equations which represented the motor under high speed operations. The dynamic behaviour of the step motor is in general non-linear. Consequently it was inadequate to approximate its performance by linear models. The solutions to these equations were therefore achieved by a computer simulation. In the past, analogue computer simulations have been attempted, however these have proven only practical for single step performance studies and for multiple stepping would prove to be extremely tedious. On the other hand a digital computer overcomes this problem and offers a great deal of flexibility. The Model represented the winding voltage equations, expressions for the developed torque, and the dynamic equations. Hysteresis and eddy currents were neglected as a linear magnetic circuit could be assumed for the particular motor under test. The equations used were those derived by Hughes and Lawenson ref 3 and Ellis ref 4 with the exception of the motion dynamics which were modified to include windage torque. Deriving the model constants from basic principles was found to be impracticable as the motor parameters required for such analysis were commercially confidential and therefore any such constants were found experimentally. Figure 9 shows the basic structure of the computer program which consists of six main blocks; torque; current; load dynamics; back-emf; phase equations and winding logic. Although the model represented only a 4 - phase stepper the program had been written to enable the investigation of the various drive modes (4A, 4B, or 4AB) and the introduction of a phase shift to obtain the minimum current condition. Details of the program and the derivations of the equations are presented in ref 1. Both the Back-emf and current equations are controlled by the phase equations which were fed into the forward loop by multipliers. The winding logic block determined which phase, or pair of phases are energised depending on the rotor magnet position, any phase advance and the selected drive mode. Each winding voltage is derived from the sum of the controlled voltage and the appropriate Back-emf voltage. The corresponding winding current is then calculated and depending on the winding logic and phase equations produced the total instantaneous current. From the instantaneous current the developed torque was computed, and hence the output speed. The Dynamic Equation Block included windage torque and load constraints and was given by

$$Td = J\ddot{\Theta} + Kw\dot{\Theta} + Tm$$

where Td is the developed torque.

J is the total inertia of the rotor and load

Tm the motor friction torque, which includes all decelerating torques, other than rotor windage.

Kw is a constant obtained experimentally and expresses the relationship between windage torque and motor speed for a given set of load dimensions.

The viscous damping terms were neglected as they are small compared with the motor friction.

The simulation model predicted that at high speeds there would be a high power consumption due to the windage. However under vacuum conditions the windage would be dramatically reduced and as confirmed by experiments at 1 torr the running torque was reduced to only that due to the motor friction torque.

5.0 THE GEMS CHOPPER MECHANISM

In 1971-72 a preliminary system study of a temperature sounding radiometer for a Geostationary Environmental Meteorological Satellite (GEMS) was performed for the UK Meteorological Office. The radiometer was to determine the temperature profile of the troposhere and low stratosphere over partially clouded as well as clear areas. In addition the instrument could determine water vapour in the lower troposhere and the total ozone concentration both for temperature sounding correction and for the purpose of ozone detection alone. The radiometer measured radiance in eleven spectral channels, six in the CO_2 absorption band, two in atmospheric window region, two in atmospheric water absorption regions and one in the ozone absorption band. Cadmium Mercury Telluride detectors were specified with passive radiation cooling. The optical arrangement is based on a 20 cm aperture Cassegrain telescope with a large moveable plane mirror to perform the required scanning. The field of view of the instrument was 113 km diameter for the high altitude channels and 34 km for each sub-field of the remaining channels. Modulation being achieved by a reflecting chopper blade giving alternate space/earth views. The chopper mechanism as shown in fig. 10 comprises a 14 cm diameter disc with 30 slots. The chopper was to rotate at a uniform speed of 2000 rpm over a 5 year period in space. As the motor requirement was that it must be small, light, efficient, reliable and easily driven, the self-commutating stepper motor was chosen as the optimum drive. The drive motor assembly would incorporate dry lubricated bearings and if required, additional reliability would be assured by the inclusion of redundant bearings and stepper motor. Work carried out by the MSDS Tribology Group on lead lubricated bearings (ref. 3) predict single bearing reliability of 0.935 for a 5 year mission at 2000 rpm. This result being extrapolated from bearings having completed 10 years life at 3000 rpm at pressures of 10^{-10} torr.

CONCLUSION

The M.Sc. Project demonstrated that a self-commutating permanent magnet stepper motor could be adapted to operate as a brushless d.c. motor. Several motor drive techniques were investigated and the development of several commutating and tachometer techniques established two final brushless designs. A low speed motor ($<$ 2000 rpm) using reed-switches and a magnetic shunt and a high speed motor using Hall Effect elements. Both these motors used an inertialess tacho utilising the motor back-e.m.f.. The experimental results verified that the self-commutating stepper motor has the same output performance as a d.c. motor, and demonstrated that the final design provided a very high speed d.c. motor with an efficiency of better than 70%. The study of the torque and back-e.m.f. performance and the establishment of enhancing the motor performance by a phase advance technique contributed to the success of this motor design. Also although the aim of the project was to achieve a speed of 20,000 rpm, a no-load speed of 32000 rpm was recorded during the performance test. The most significant advantage that this self-commutating motor has over other commercially available brushless motor is that it is fabricated from a motor available from many manufacturing sources. The simplicity of the drive, commutation and tacho ensures reliability, and the high speed and efficiency capability makes this motor a low cost rotary device, suitable for high speed applications in a space environment. Apart from the development of a novel brushless motor it is believed that the operation of a stepper motor at speeds in excess of the 'drop-out' rate is an important contribution to the knowledge of stepper motor technolog

ACKNOWLEDGEMENTS

The author would like to thank Dr. L. Mansi University of Surrey, Mr. D. Steward MSDS whom originally inspired the self-commutating stepper motor and L. Kozuchowski of Moore Reed whose knowledge and test equipment provided invaluable assistance. Thanks are also due to the Technical Director of GEC - Marconi Electronics Ltd. for permission to publish this paper.

REFERENCES

ref 1 Design and Performance of a self-commutating High Speed Stepper Motor. K. Dalley, M.Sc. Thesis, University of Surrey. Sept. 77.

ref 2 A Preliminary System Study of a Temp. Sounding Radiometer for a Geostationary Met. Sat. Marconi Report reference 28053 Dec. 72.

ref 3 Electromagnetic damping in stepping motors.
A Hughes and P.J Lawrenson.
Proc. IEE Vol. 122 No. 8 August 1975.

ref 4 Analysis and Control of Permanent-Magnet Stepper Motor.
P.J Ellis.
The Radio and Elec. Eng. Vol. 41 No. 7 July 1971.

ref 5 Lubrication by Lead Films. A survey of existing and proposed applications.
P.J. O'Donnell ESA SP111 1st Space Tribology Symp. Oct. 75.

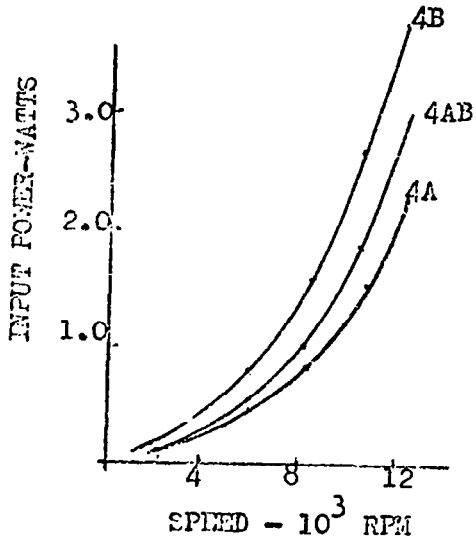

FIG. 1 DRIVE MODE CHARACTERISTICS

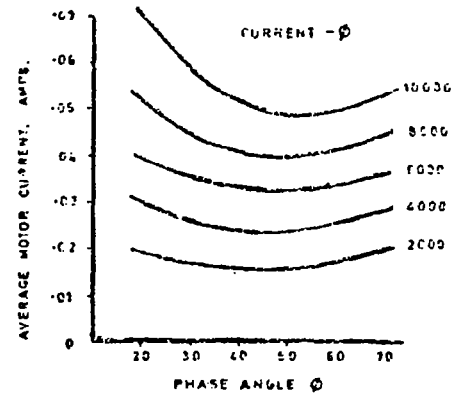

FIG. 2 PHASE SHIFT CHARACTERISTICS

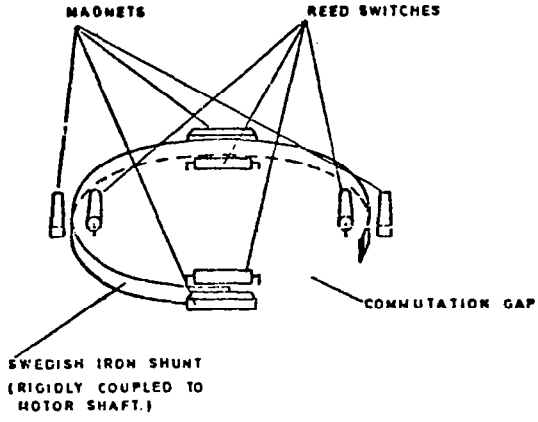

FIG. 3 REED SWITCH POSITION SENSOR

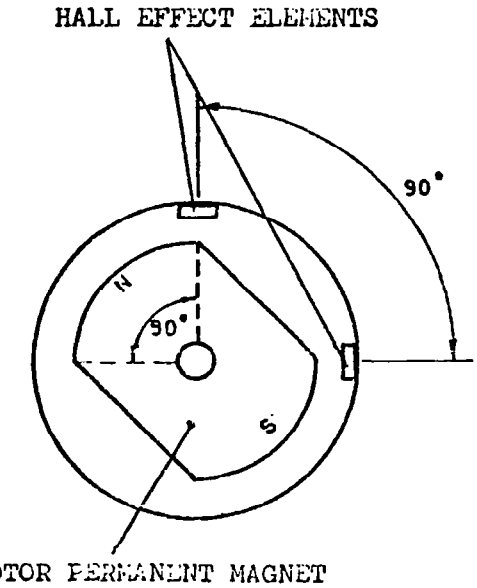

FIG. 4 THE HALL EFFECT SENSOR

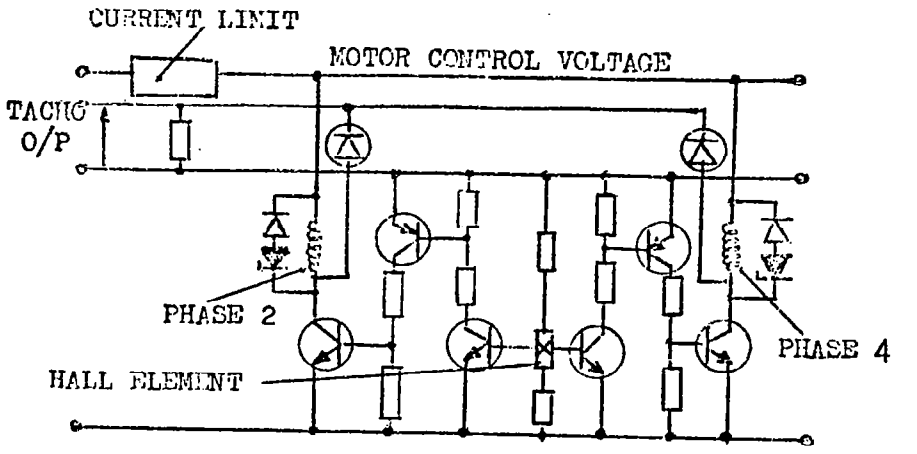

FIG. 5

BASIC DRIVE CIRCUIT

(PHASE 2 & 4 ONLY)

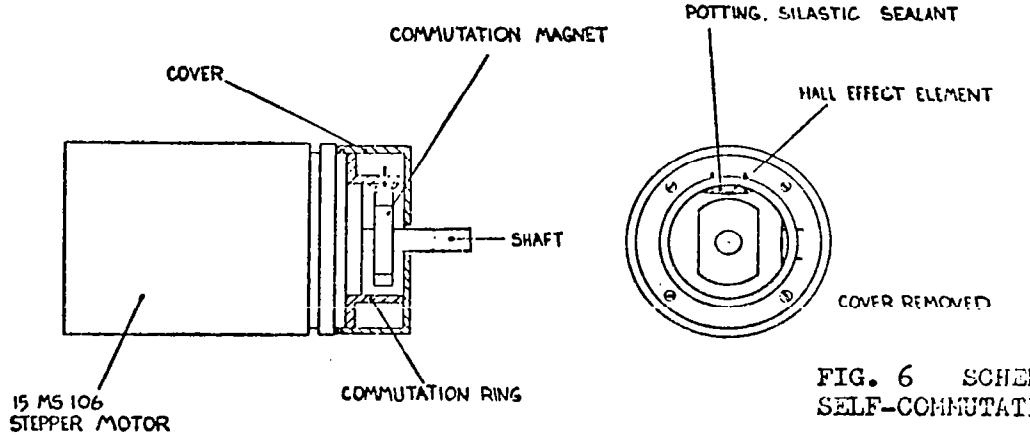

FIG. 6 SCHEMATIC OF THE SELF-COMMUTATING STEPPER *

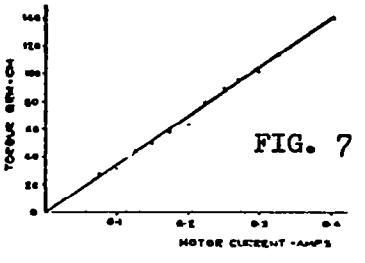

FIG. 7

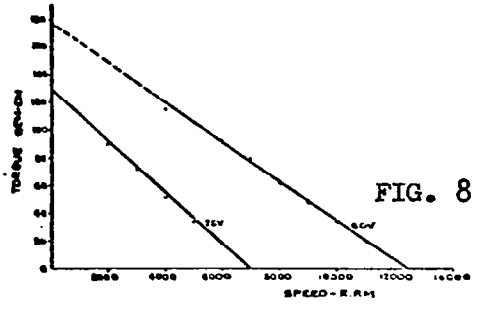

FIG. 8

MOTOR TORQUE PERFORMANCE

* For the M.Sc. project the Hall Elements were externally mounted.

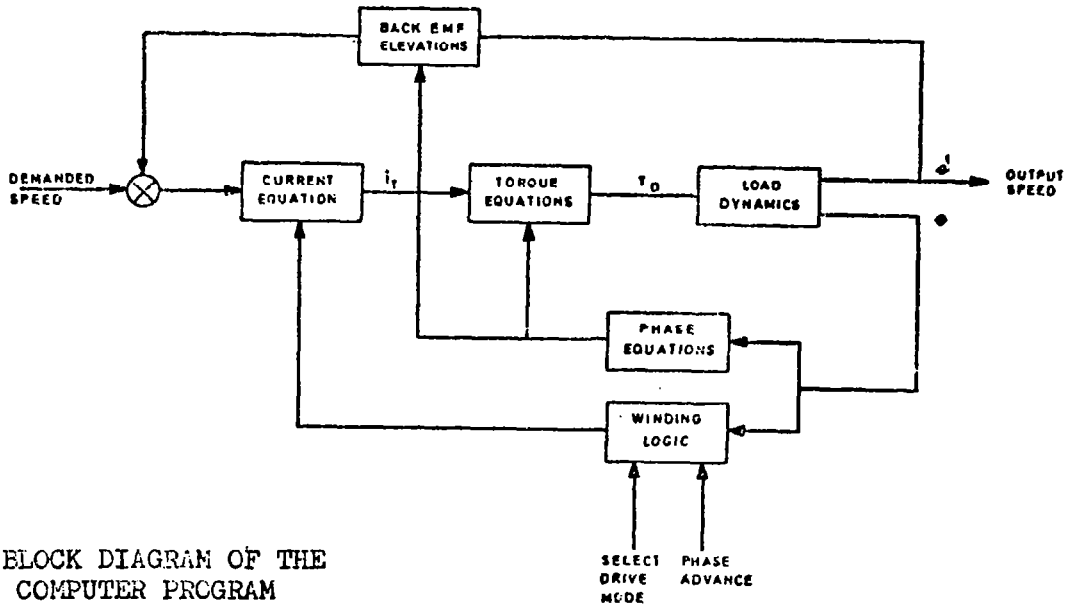

FIG. 9 BLOCK DIAGRAM OF THE COMPUTER PROGRAM

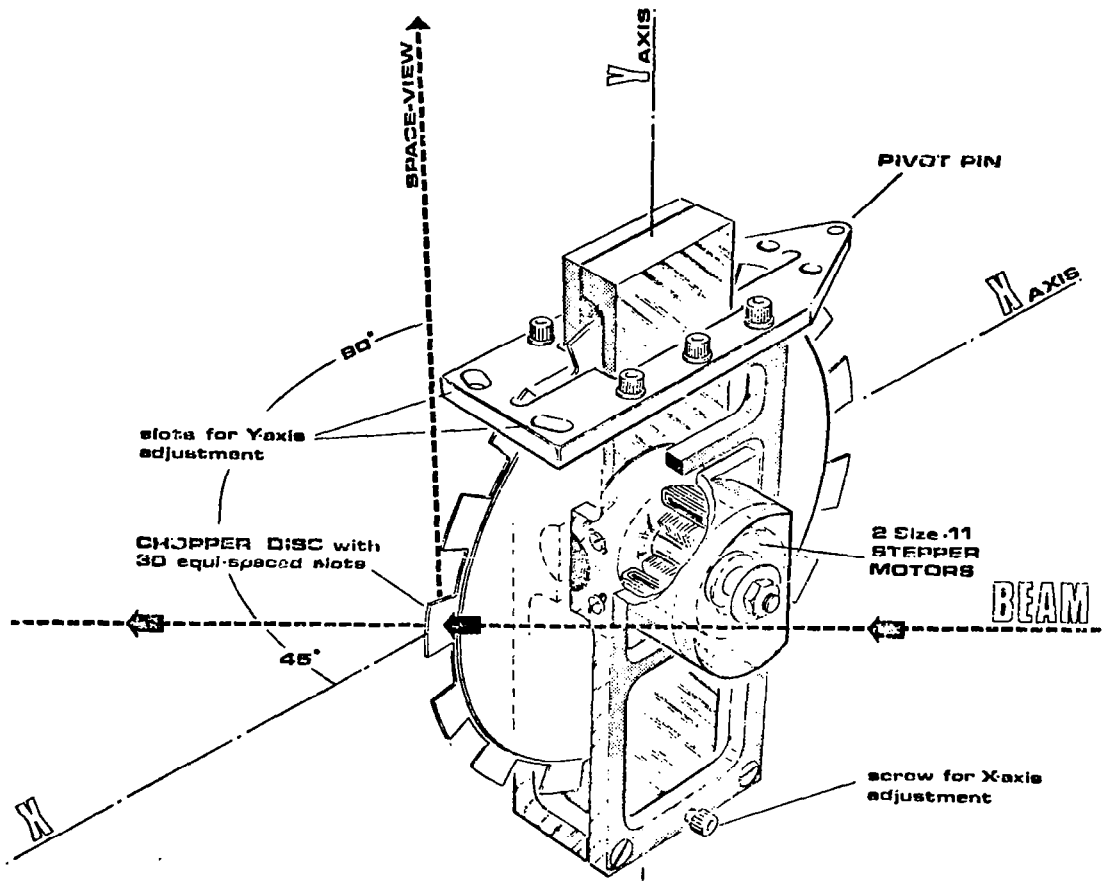

FIG. 10 GEMS CHOPPER MECHANISM